Journal of Alloys and Compounds 488 (2009) 260–264

Contents lists available at ScienceDirect

Journal of Alloys and Compounds

journal homepage: www.elsevier.com/locate/jallcom

Effect of active heterogeneous nucleation particles on the grain refining efficiency in an Mg–10 wt.% Y cast alloy

D. Qiu[a,*], M.-X. Zhang[a,b]

[a] School of Mechanical and Mining Engineering, the University of Queensland, Brisbane, Qld. 4072, Australia
[b] ARC Centre of Excellence for Design in Light Metals, Brisbane, Australia

ARTICLE INFO

Article history:
Received 20 April 2009
Received in revised form 17 August 2009
Accepted 22 August 2009
Available online 28 August 2009

Keywords:
Magnesium alloys
Casting
Grain refinement
Heterogeneous nucleation

ABSTRACT

Addition of pure Al into the melt of an Mg–10 wt.% Y cast alloy leads to in situ formation of Al_2Y particles. Part of these particles can act as heterogeneous nucleation sites and reduce the grain size. Such particles are termed active nucleation particles. In this paper, grain refining efficiency of the Al_2Y particles was experimentally studied in terms of the number density and size of the total and active Al_2Y particles. The results show that the as-cast grain size is closely related to the number density of the active particles ρ_a that is controlled by the size of active particles, d_{ap}, at different Al addition levels. The finest grains were achieved at 2 wt.% Al addition level, which corresponds to the average d_{ap} of 6–6.5 μm with ρ_a of 260–290 /mm^2. The active particle size effect was discussed based on the competitive processes between heterogeneous nucleation and crystal growth, both of which are associated with the curvature undercooling.

1. Introduction

Grain refinement by inoculating heterogeneous nucleation particles can effectively improve the quality of castings and mechanical properties of foundry alloys [1]. One of the most successful examples of this approach is the application of Al–Ti–B master alloys in aluminium alloys, in which either the TiB_2 or the Al_3Ti or both types of particles act as heterogeneous nucleation sites or so called inoculants [2–4]. However, not all particles in the melts can promote the heterogeneous nucleation. Following Maxwell and Hellawell's hypothesis [5] that the final grain size is a result of competition between heterogeneous nucleation and crystal growth, Greer and co-workers [4,6–8] developed a free growth model and a numerical method to predict the grain size in Al casting alloys. The good agreement of the predictions with the experimental results indicated that only those particles, of which the size is large enough, can effectively inoculate the metals. This sort of particles is called active nucleation particles. However, the effect of the active nucleation particles on grain refinement efficiency has not been fully addressed previously. In the past nearly half century, extensive research has been focused on developing new grain refiner for Mg cast alloys, and a number of grain refiners have been reported, such as Zr for Al/Si/Mn-free Mg alloys [9] and Al_4C_3 [10–12], SiC [13–15] etc. Although the dependence of grain refining efficiency on the addition level of inoculated particles has been investigated [11,12,15,16], there is still lack of understanding the actual role of the active particles in grain refinement. Only limited information can be found in the report of Ma and his co-workers [17]. They observed that not all Zr particles contribute to the grain refinement in pure Mg and the active Zr particle size is around 2 μm at 1 wt.% Zr addition level.

Easton and StJohn [18] reported that the grain size of the as-cast Al alloys is closely related to the number density of active TiB_2 particles in the melt. Suppose the number density of total inoculated particles is ρ, and the fraction of active particles is f_a, the number density of active nucleation particles ρ_a can be expressed as follows:

$$\rho_a = \rho f_a. \quad (1)$$

Normally the fraction of active particles is very small. A typical value of f_a is 1–2% in an Al–Ti–B master alloy used in Al alloys [19]. Furthermore, the grain refining efficiency of nucleation particles also depends on the size of the particles. Perepezko [20] indicated that the critical undercooling of nucleation, ΔT_n, is inversely proportional to the diameter of spherical nucleation particle, d_p:

$$\Delta T_n = \frac{4\gamma_{SL}}{(d_p S_v)}, \quad (2)$$

where γ_{SL} is the interfacial energy between liquid and nucleation particles and S_v is entropy of fusion of the nucleation per unit volume. In the above equation, d_p can also approximately represent the size of polygonal particles [21]. Eq. (2) predicts that heteroge-

* Corresponding author. Tel.: +61 733 65 3987; fax: +61 733 65 3888.
E-mail address: d.qiu@uq.edu.au (D. Qiu).

0925-8388/$ – see front matter © 2009 Elsevier B.V. All rights reserved.
doi:10.1016/j.jallcom.2009.08.100

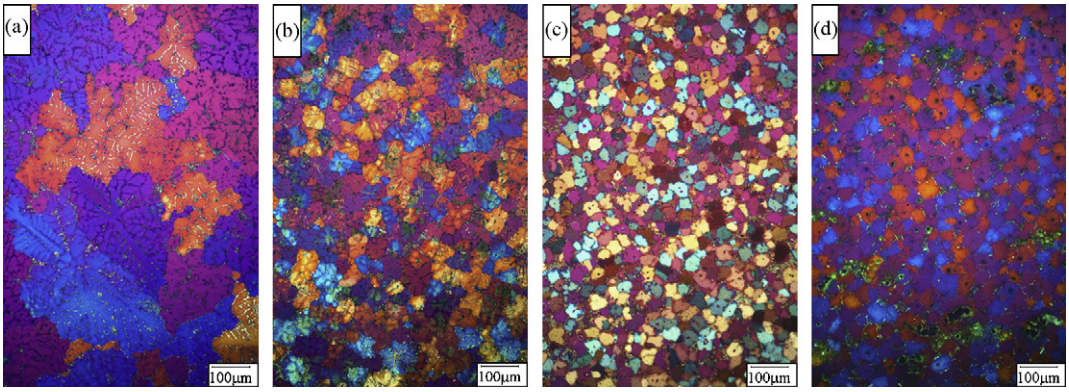

Fig. 1. Optical micrographs of as-cast Mg–10 wt.% Y alloy at: (a) 0.5 wt.% Al (base alloy); (b) 0.6 wt.% Al; (c) 2 wt.% Al and (d) 3 wt.% Al addition.

neous nucleation more easily occurs on larger particles than on smaller ones. This implies that the larger particles have higher nucleation activity, which may lead to smaller grains. But, this is not always true because grains nucleated on larger particles tend to grow faster due to smaller curvature undercooling. Hence, in a specified alloy system, there must be an optimum size of active nucleation particles that produce the finest grains.

Recently, we have reported a new and effective grain refiner – Al_2Y that formed in situ in an Mg–10 wt.% Y cast alloy through addition of pure Al [22]. Two reproducible crystallographic orientation relationships between the active nucleation particles and the Mg matrix have been identified using electron back scatter diffraction (EBSD) technique [23]. This indicates the high activity of Al_2Y particles as heterogeneous nucleation sites. But, the effect of physical natures, such as the size, number density and fraction of the active Al_2Y particles, on the grain refining efficiency is still beyond understanding. Hence, the present work aims to investigate how the Al addition affects the grain refining efficiency; to study the variation of the number density and size of the total and the active Al_2Y particles formed in situ with the addition of Al; and to understand the effect of number density and size of active Al_2Y particles on grain refining efficiency in an Mg–10 wt.% Y cast alloy.

2. Experimental

About 1 kg Mg–10 wt.% Y base alloy was firstly molten in a BN coated mild steel crucible at 730 °C under a protective atmosphere of mixed CO_2 and SF_6 in dry air. Pure Al (99.7%) was added into the melt in the amounts from 0.5 wt.% to 3.0 wt.% and inoculated for 30 min before casting. The minimum Al addition level applied because only the Al addition on top of 0.5 wt.% leads to the in situ formation of Al_2Y particles and results in grain refinement [22]. Extra pure Y (98.6%) was also added simultaneously in terms of the stoichimetric ratio of Al_2Y to compensate the amount of Y consummated due to the formation of the intermetallic compound. Thus, the solute concentration, 10 wt.% Y, can be retained in the melt. Then, the melt was cast into a cylindrical steel mould (Ø20 mm × 180 mm) that was preheated in oven at 250 °C. Block samples were cut from the ingot at section that is 20 mm away from the top. Metallographic samples were etched by an acetic–picric solution after well polishing. The grain size at the centre of transverse sections was examined by the line-intersect method under polarised light. The Al_2Y particles sitting within the fine Mg grains in the as-cast samples are regarded as the possible active heterogeneous nucleation sites or inoculants. Since the active nucleation particles are always crystallographically related to the metal matrix [24], one or more reproducible orientation relationships (OR) between the active nucleation particles and their metal matrix should be observed. The ORs was examined using back scattered electron diffraction (EBSD) facility equipped in a JEOL 6460 LA scanning electron microscopy (SEM). All other Al_2Y particles are considered as inactive nucleation particles. These include the Al_2Y particles that are within the Mg grains, but have random or non-reproducible ORs and the small particles sitting along grain boundaries. Each active nucleation particle was numbered and its size was measured once it has been verified by crystallographic examination in terms of the ORs between the particles and Mg matrix. The statistical result of the number density and size distribution of the total Al_2Y particles were obtained by ex situ measurement through ImageTool© software.

3. Results

Fig. 1 shows the optical micrographs of the as-cast samples at different addition levels of Al. It can be seen that increasing the addition level of Al from 0.5 wt.% to 0.6 wt.% not only significantly reduces the grain size, but also leads to the formation of equiaxed grains. The grain size of the base alloy with 0.5 wt.% Al addition shown in Fig. 1(a) is about 210 μm. Previous study [22] has proved that there is no Al_2Y present in this base alloy and the entire 0.5 wt.% Al added has been dissolved in the liquid, of which the solubility is 0.5 wt.%. Adding 0.1 wt.% Al more into the melt of the base alloy sharply decreases the grain size to 55 μm, as shown in Fig. 1(b). The finest grains that have average grain size of 27 μm were obtained at 2 wt.% Al addition as shown in Fig. 1(c). However, more than 2 wt.% addition of Al does not further refine the grains, but slight coarsening occurs. The grain coarsening at 3 wt.% Al addition can be observed in Fig. 1(d). The variation of Mg grain size with Al addition level is also presented in Fig. 2. The L-shape curve of the grain size associated with the grain refiner addition level is quite similar to the observations from Al_3Ti/TiB_2 in Al alloys [6] and Zr in Al-free Mg alloys [16]. This implies that the grain refining efficiency of Al_2Y is compelling.

The number density of active nucleation particles, ρ_a, and of the total Al_2Y particles, ρ, was evaluated in three rectangular areas that are close to the centre of transverse section of each sample. The rectangles are 600 μm long and 400 μm wide. The values of ρ_a and ρ measured at different Al addition levels are presented in

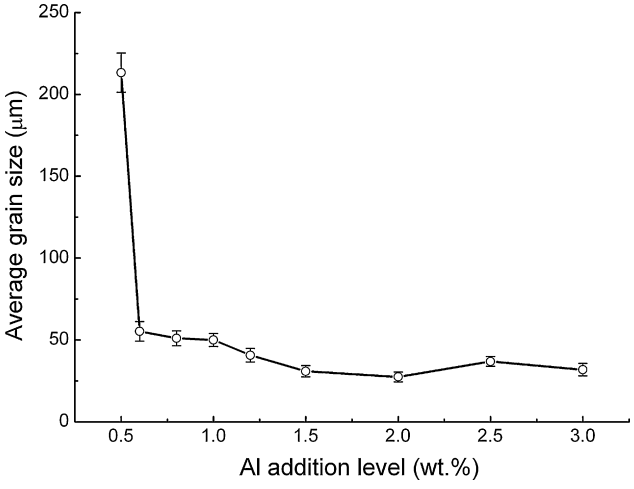

Fig. 2. The grain size of Mg–10 wt.% Y alloy at different Al addition levels.

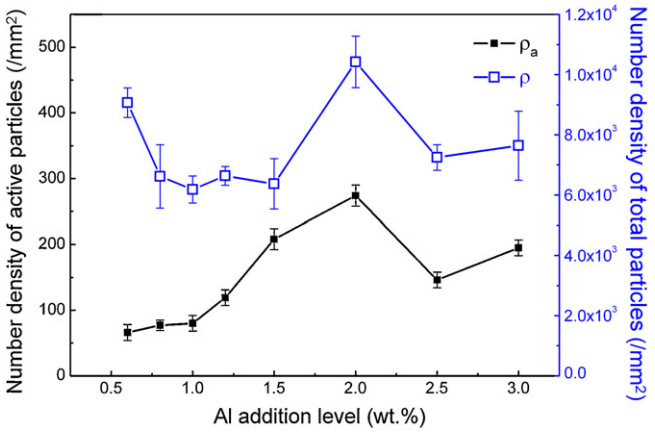

Fig. 3. The number density of total Al_2Y particles, ρ, and the number density of active nucleation particles, ρ_a at different Al addition levels.

Fig. 3, in which the left *y*-axis is for ρ_a and the right *y*-axis is for ρ. It can be seen that the ρ_a value increases with addition of Al and the highest value is about 260–290 /mm^2 that achieved at 2 wt.% Al addition. Then the ρ_a value reduces with addition of Al. This result shows that the grain size of the as-cast Mg alloy is closely related to the number density of the active nucleation particles. However, the variation of ρ value with Al addition level is opposite to ρ_a value when the addition level is lower than 1.5 wt.%. In addition, Fig. 3 also indicates that the average number density of the active nucleation particles is only 1–2% of the number density of the total particles. The rest of Al_2Y particles do not significantly contribute to grain refinement.

In order to further understand the influence of Al_2Y particles on the grain refinement, we also examined the particle size distribution of the total Al_2Y particles, d_p, and of the active nucleation particles, d_{ap}. The results are shown in Figs. 4 and 5, respectively. About 40% of the total Al_2Y particles are around 2 μm in diameter. However, the size of the majority of active nucleation Al_2Y particles increases from around 3.5 μm to 6 μm as the Al addition level rises from 0.6 wt.% to 1.5 wt.%. In addition, near Gaussian distribution of active particle size can be clearly observed for each addition level. At 0.6 wt.% Al addition level, most of the active nucleation Al_2Y particles are relatively small, ranging from 1 μm to 5 μm. The active nucleation particles are getting bigger and some exceed 10 μm with the increasing Al additions. However, when the Al addition is over 1.5 wt.%, the evolution of the distribution profiles slows down. Fig. 6(a–c), shows the typical back scattered electron images of the active Al_2Y particles within Mg grains as pointed by the arrows at

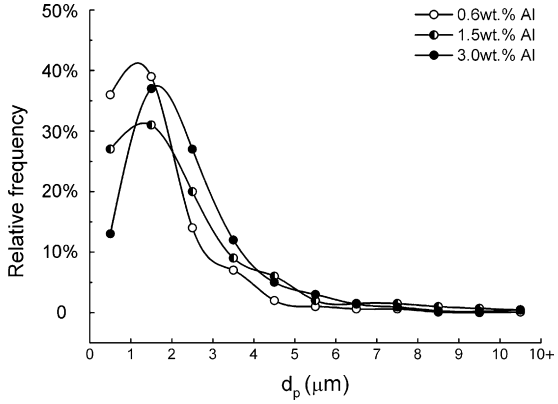

Fig. 4. The size distribution of total Al_2Y particles in refined Mg–10 wt.% Y alloy at different Al addition levels.

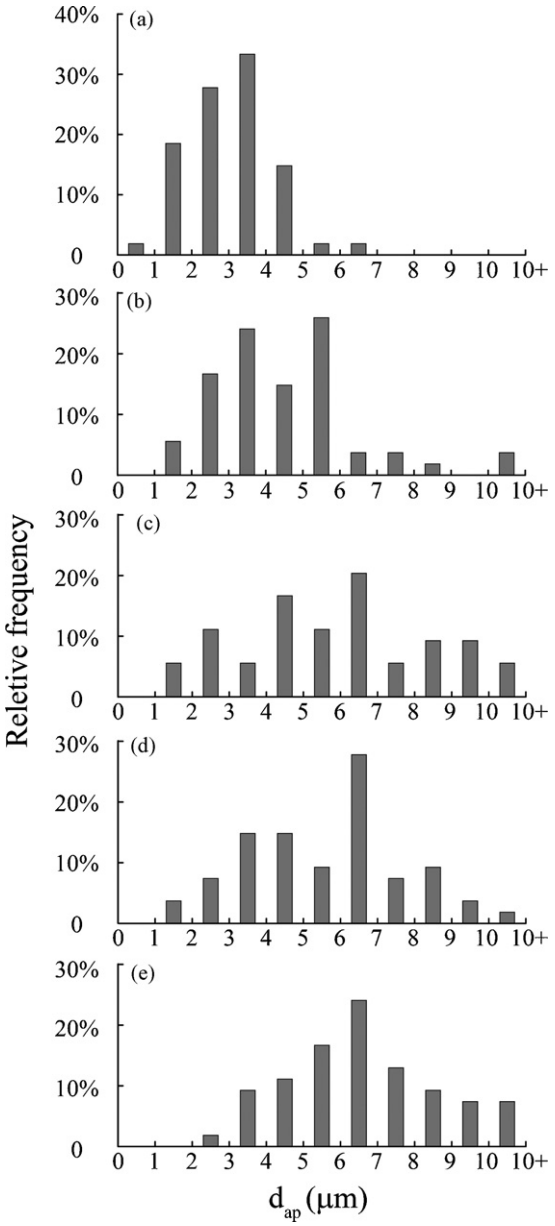

Fig. 5. The size distribution of active nucleation particles in refined Mg–10 wt.% Y alloy at: (a) 0.6 wt.% Al; (b) 1 wt.% Al; (c) 1.5 wt.% Al; (d) 2 wt.% Al and (e) 3 wt.% Al addition.

Al addition levels of 0.6 wt.%, 2.0 wt.% and 3.0 wt.%, respectively. It is clearly shown in Fig. 6 that all the active Al_2Y nucleation particles are in polygonal morphology, and located close to the centre of grains. They are also normally bigger than the inactive grain boundary particles.

The relationship between the mean particle size and the Al addition level is shown in Fig. 7. The average size of total Al_2Y particles, d_p varies from 1.6 μm at 0.6 wt.% Al addition to 2.0 μm at 1.0 wt.% Al addition, then tends to be constant up to 3.0 wt.% Al addition. In contrast, the mean particle size of the active nucleation particles is much more sensitive to the Al addition. The average value of d_{ap} rises from 3.5 μm at 0.6 wt.% Al addition to 6.5 μm at 1.5 wt.% Al addition. It is stabilized at 6 μm at 2.0 wt.% Al addition and then slowly increases to 7 μm at 3 wt.% Al addition. In consideration of the results in Figs. 1 and 2, it is concluded that the most effective size of active Al_2Y nucleation particles for ~10 wt.% Y Mg alloy is 6–6.5 μm. The Al_2Y particles that are smaller than 2 μm do not contribute to any grain refinement.

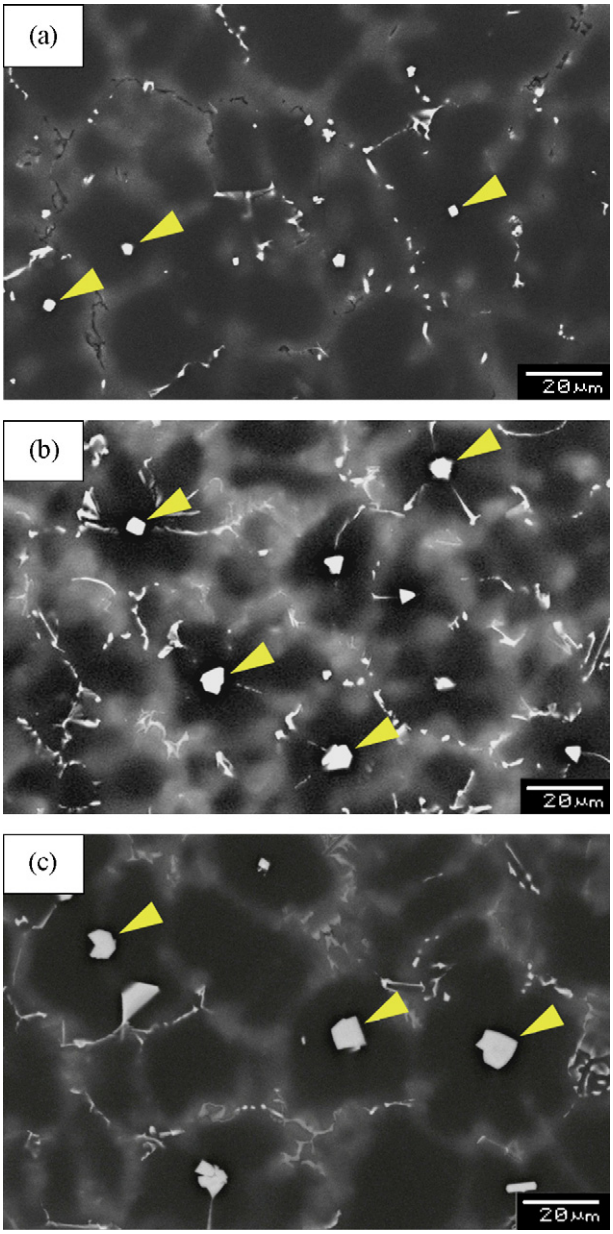

Fig. 6. Back scattered electron images of active Al_2Y nucleation particles in refined Mg–10 wt.% Y alloy at (a) 0.6 wt.% Al; (b) 2 wt.% Al and (c) 3 wt.% Al addition.

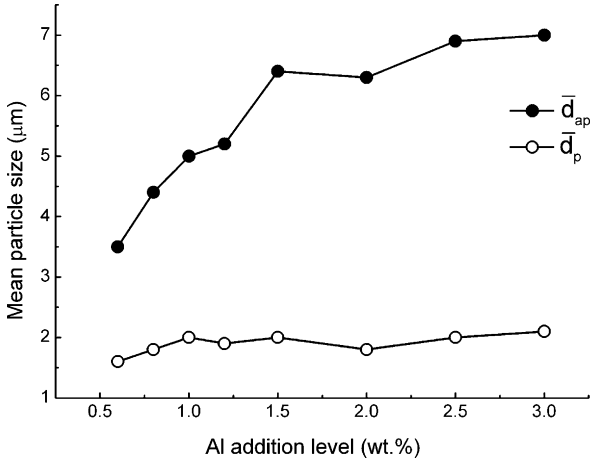

Fig. 7. The mean particle size of the total Al_2Y particles $\bar{d}_p$ and of the active nucleation particles $\bar{d}_{ap}$ at different Al addition levels.

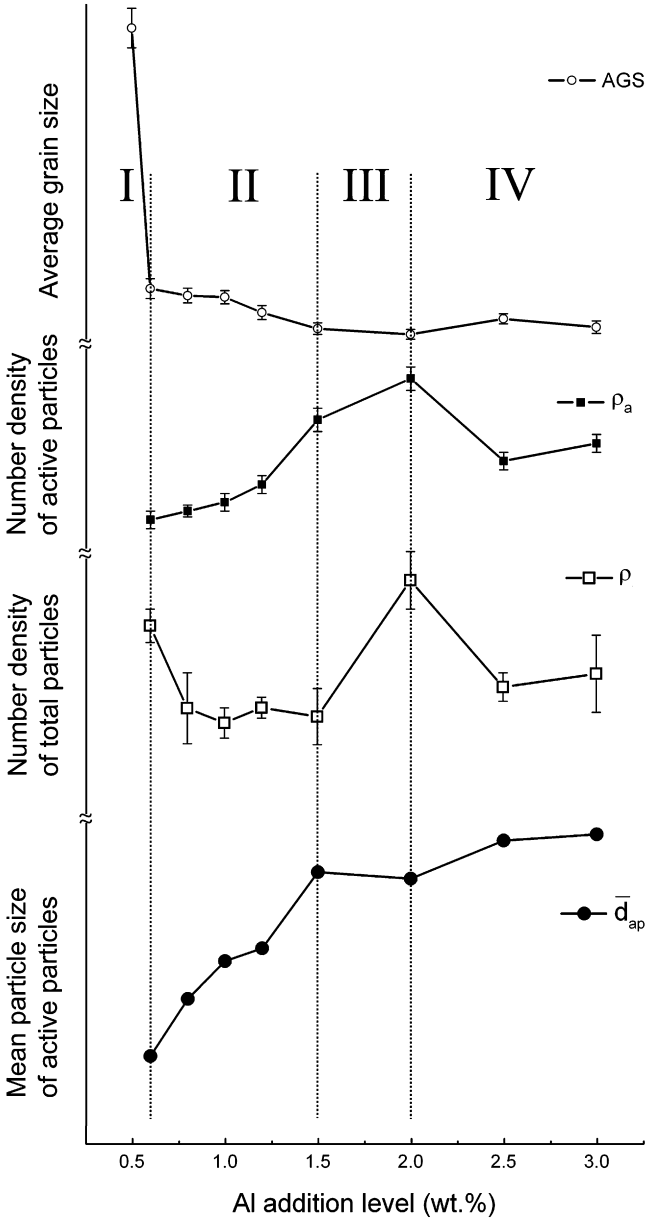

Fig. 8. The integrated graph showing the dependence of the average grain size (AGS) on the number density of active and total Al_2Y particles, ρ_a and ρ, and the mean particle size of active nucleation particles, $\bar{d}_{ap}$.

4. Discussion

To understand the effect of Al addition on the grain size of cast Mg–10 wt.% Y alloy, Figs. 2, 3 and 7 are combined into one figure as shown in Fig. 8. One can clearly observes that the most significant reduction of grain size occurs between 0.5 wt.% and 0.6 wt.% Al addition (Phase I). Because there is no Al_2Y can be detected at 0.5 wt.% Al addition [22], this result implies that once Al_2Y particles form in situ in the melt at the addition level of 0.6 wt.% Al, heterogeneous nucleation on Al_2Y particles takes place, which results in grain refinement. Further reduction of grain size relies on the average size, d_{ap}, and number density, ρ_a, of the active Al_2Y particles. Adding more Al into the melt produces larger amount of Al_2Y phase through increase of either the number density or the size of Al_2Y particles or both. Results showing in Fig. 8 indicate that increase Al addition from 0.6 wt.% to 1.5 wt.% (Phase II) tends to produce more big particles that are the potential active nucle-

ation sites. As a result, the number density of active particles, ρ_a, increases though bigger particles were produced at the scarification of number density of total particles, ρ. Adding more Al to 2.0 wt.% (Phase III), the Al_2Y particle size gets stabilized so that the number densities of both active particles and inactive particles increase with the increasing Al additions, and hence, finer grains were obtained. However, once the addition of Al is over 2.0 wt.% (Phase IV), the fraction of even coarser particles keeps increasing. This not only lowers the number density of both active and inactive particles, but also leads to grain coarsening as shown in Fig. 1(d).

The present results and previous work [18] indicate that the number density and size of active particles play the key roles in grain refinement. The effect of number density is straightforward since more active nucleation particles normally lead to finer grains. The size effect is explained as follows: As proposed by Maxwell and Hellawell [5] and Greer et al. [6], the final grain size of castings is associated with the competitive processes between nucleation and growth. Both processes are affected by the actual undercooling, ΔT, which corresponds to the constitutional undercooling ΔT_C deducting the curvature undercooling ΔT_n. In the present work, addition of Al is combined with simultaneous addition of Y according to the atomic ratio of Al to Y in Al_2Y, so that the actual solute concentration in the melts is constant after the formation of Al_2Y in all samples. It means that the effect of ΔT_C resulting from the solute atom segregation can be considered as the same for all as-cast samples. Therefore, the different grain sizes of the samples at various Al addition levels are mainly caused by the curvature undercooling, ΔT_n. According to Eq. (2), when the heterogeneous nucleation occurs on a larger particle, the nucleus may have larger diameter, d_{ap}. Such nucleus corresponds to smaller curvature undercooling, ΔT_n, and results in a larger actual undercooling, ΔT. Therefore, higher nucleation rate can be achieved, which leads to grain refining. However, the larger ΔT will also raise the growth rate of new crystals and lead to the more latent heat release per unit time. It will in turn stifle or even terminate the nucleation event until $\Delta T \leq 0$. This effect will negatively contribute to the grain refinement. As a result of these two competing processes, there is a optimum size of the active nucleation particle, which leads to the finest grains. In the present work, the optimum size of Al_2Y particles to achieve the highest grain refining efficiency is 6–6.5 μm in the Mg–10 wt.% Y alloy. This conclusion is consistent with the prediction through Greer's numerical approach [6–8,15], of which an optimum mean particle size is accessible for the highest grain refining efficiency. More importantly, the optimum value of the active nucleation particle size based on the current experimental results provides a more straightforward guidance for optimizing the grain refinement process in future castings.

5. Summary

1. Addition of 0.6 wt.% Al into Mg–10 wt.% Y cast alloy dramatically reduces the as-cast grain size from 210 μm to 55 μm, and the finest grains of 27 μm were obtained at 2.0 wt.% Al addition level.
2. There is only 1–2% of the total Al_2Y particles formed in situ in the melt contributes to grain refinement. The number density and size of these active nucleation particles play an important role in grain refining efficiency.
3. Although the mean size of active Al_2Y nucleation particles increases with Al addition, the highest number density of the active particles can only be obtained at 1.5–2.0 wt.% Al additions, which produces the finest Mg grains.
4. The optimum size of active Al_2Y nucleation particles corresponding to the most effective grain refinement for Mg–10 wt.% Y cast alloy is 6–6.5 μm. In general, Al_2Y particles that are smaller than 2 μm do not act as heterogeneous nucleation sites.

Acknowledgement

Authors are very thankful to the Australian Research Council and the ARC Centre for Design in Light Metals for funding supports.

References

[1] D.G. McCartney, Int. Mater. Rev. 34 (1989) 247.
[2] B.S. Murty, S.A. Kori, K. Venkateshwralu, R.R. Bhat, M. Chakraborty, J. Mater. Process. Technol. 89–90 (1999) 152.
[3] M.A. Easton, D.H. StJohn, Acta Mater. 49 (2001) 1867.
[4] W.A. Schneider, T.E. Quested, A.L. Greer, P.S. Cooper, in: N. Crepeau (Ed.), Light Metals, vol. 2003, TMS (The Minerals, Metals & Materials Society), 2003, p. 953.
[5] I. Maxwell, A. Hellawell, Acta Metall. 23 (1975) 229.
[6] A.L. Greer, A.M. Bunn, A. Tronche, P.V. Evans, D.J. Bristow, Acta Mater. 48 (2000) 2823.
[7] A. Tronche, A.L. Greer, in: R.D. Peterson (Ed.), Light Metals 2000, TMS, Warrendale, PA, 2000, p. 827.
[8] T.E. Quested, A.L. Greer, Acta Mater. 52 (2004) 3859.
[9] E.F. Emley, Principles of Magnesium Technology, Springer, Oxford, 1966, p. 200.
[10] L. Lu, A.K. Dahle, D.H. StJohn, Scripta Mater. 53 (2005) 517.
[11] T. Motegi, Mater. Sci. Eng. A 413–414 (2005) 408.
[12] G. Han, X.-F. Liu, H.-M. Ding, J. Alloys Compd. 467 (2009) 202.
[13] A.K. Dahle, Y.C. Lee, M.D. Nave, P.L. Schaffer, D.H. StJohn, J. Light Met. 1 (2001) 61.
[14] M.A. Easton, A. Schiffl, J.-Y. Yao, H. Kaufmann, Scripta Mater. 55 (2006) 379.
[15] R. Günter, C. Hartig, R. Bormann, Acta Mater. 54 (2006) 5591.
[16] Y. Tamura, T. Motegi, J. Light Met. Weld. Construct. 47 (1997) 679.
[17] Ma Qian, D.H. StJohn, M.T. Frost, Scripta Mater. 50 (2004) 1115.
[18] M.A. Easton, D.H. StJohn, Metall. Mater. Trans. A 36A (2005) 1911.
[19] J.H. Perepezko, In Metals Handbook, vol. 15, ninth ed., ASM, Materials Park (OH), 1988, pp. 101–108.
[20] W. Kurz, D.J. Fisher, Fundamentals of Solidification, 4th ed., Trans Tech Publications Inc., Switzerland, 1998.
[21] S.A. Reavley, A.L. Greer, Philos. Mag. 88 (2008) 561.
[22] D. Qiu, M.-X. Zhang, J.A. Taylor, P.M. Kelly, Acta Mater. 57 (2009) 3052.
[23] D. Qiu, M.-X. Zhang, P.M. Kelly, Scripta Mater. 61 (2009) 312.
[24] D.A. Porter, K.E. Easterling, Phase Transformations in Metals and Alloys, Chapman & Hall, London, 1992.